Vehicle Related Influence of Post-Car Impact Pedestrian Kinematics on Secondary Impact

Michael Hamacher [1] , Lutz Eckstein [2] , Ruth Paas [3]

Abstract   In this paper the pedestrian motion after the vehicle impact is thoroughly investigated within a multibody variation study. The intention of this study is to generally assess the injury risk due to secondary impact solely with the help of kinematic parameters. Pedestrian centre of gravity and rotational kinematics are analysed from the first contact up to the final position. The study shows that for most vehicles launch angle and speed as well as flying height are rather stable against variations of the initial stance and impact position. In contrast to this, the pedestrian's rotation is highly influenced by leg and arm posture, which makes predictions of head impact risk in secondary impact difficult. A high bonnet leading edge (BLE) in relation to the pedestrian stance as well as large bonnet and windshield angles increase the risk of a head impact on the ground, whereas the kinematic boundary conditions before the secondary impact influence the sliding distance. A reduction in collision speed however is beneficial for the pedestrian kinematics and leads to a decrease in altitude, rotation and throw distance. The post-car impact pedestrian kinematics as well as the influence of a reduction in collision speed is demonstrated in tests with the Polar-II pedestrian dummy.

Keywords   Multibody simulation, pedestrian kinematics, secondary impact

I. INTRODUCTION

Since the start of pedestrian to car accident research the focus has mainly been on the primary impact to the vehicle, while the pedestrian kinematics thereafter as well as ground contact conditions are still not fully understood. Grünert et al have investigated the phenomena of secondary (ground) impacts for vulnerable road users regarding the circumstances that may promote these impacts as well as their severity compared to the injuries caused by contact with the vehicle [1]. Real world accident cases have been reconstructed and additionally parametric studies examining the importance of specific causation factors have been conducted. The major result of this investigation was that on balance and compared with the first impact, a head injury caused from the second impact was less frequent and either equally serious or less serious. These findings were similar to the results of Otte et al [2]. Furthermore, parameters like the initial pedestrian position, the vehicle front shape and the impact velocity have a great influence on the head injuries attributable to secondary ground impacts. However, the number of real world accident cases considered and the range of parameters examined in the parametric studies is small. In addition the real world accident cases represented a retrospective vehicle population.

The goal of this paper, which is based on [3], is to evaluate the post-car impact pedestrian kinematics for a wide range of accident scenarios, including different current vehicle shapes, collision velocities, pedestrian sizes, impact positions and walking postures. Pedestrian centre of gravity and rotational kinematics are analysed from the first contact up to the final position. With the help of adequate kinematic parameters six different vehicle classes will be compared qualitatively regarding secondary impact for children and adults. More than one thousand MADYMO simulations have been performed, resulting in a much bigger amount of simulations than in other studies dealing with secondary impact kinematics like in the study by Grünert et al [1] or in a more recent study by Simms et al regarding the influence of vehicle shape on pedestrian ground contact mechanisms [4]. Contrary to those studies the qualitative assessment of the different vehicle classes will be solely based on kinematic parameters. Injury parameters like the HIC as well as contact forces are not integrated since there is no experimental validation data available nor are the multibody models and contact characteristics of the different pedestrian sizes and car front shapes validated for injury predictions. Furthermore, the conducted

study revealed a wide scatter of values for HIC and head contact forces, which incapacitates those parameters for a general assessment. The parameters considered instead are the probability of a secondary impact on the car (followed by a ground impact), the probability of an initial head contact on the ground, the flying height, the throw distance and the launch speed after primary impact.

II. METHODS

Computational Modelling

The influence of six vehicle classes (Compact Car, Sedan, Van, SUV, OneBox, Sports Car) on the pedestrian kinematics is examined. Those classes are based upon a categorisation, which has been developed to consider the different front designs of modern cars and their impact on pedestrian accident kinematics. For each class a representative real passenger car front has been defined and converted into MADYMO, i.e. facet surfaces have been generated based on the corresponding finite elements. Fig. 1 shows the front geometries of those class representatives. Three geometrical parameters are used for classification (Fig. 2). The first one is the height of the bonnet leading edge (BLE), which has significant influence on the accident kinematics of a pedestrian. The wrap around distance (WAD) up to the bonnet rear edge (painted blue in Fig. 2) is relevant for the location of the primary head impact relative to the vehicle front. The lower the value for this parameter, the higher is the probability for a head impact in the windscreen area. The third characteristic parameter is the bonnet angle, which has an effect on the pedestrian wrap around distances as well as the post-car impact pedestrian kinematics. The illustrated experimental vehicle (see experimental testing) represents the lower spectrum of vehicle class Sedan.
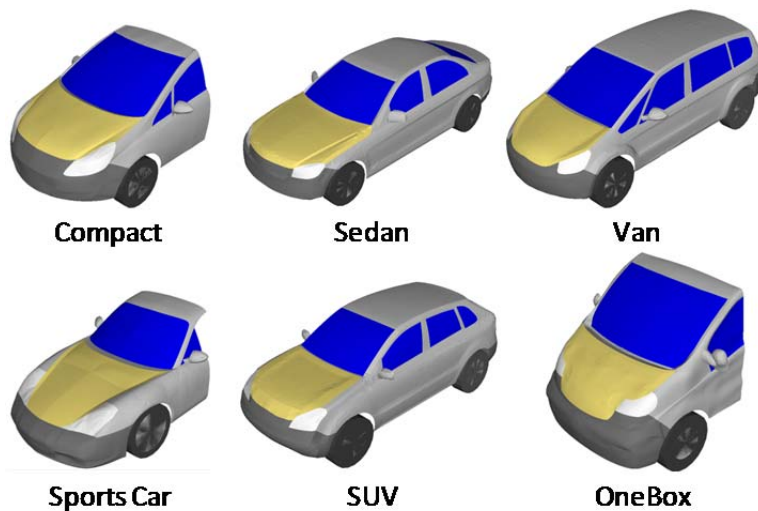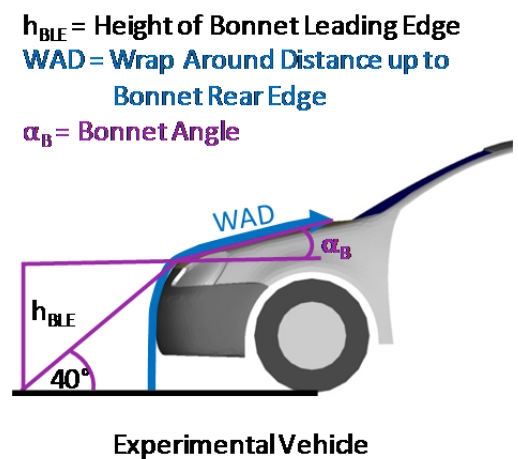

Fig. 1. MADYMO models of vehicle class representatives

Fig. 2. Geometrical vehicle parameters

The geometrical parameters of the vehicle class representatives are given in Table 1. The contact stiffness characteristics defined for the vehicle models are derived from the APROSYS-project and based on the stiffness corridors developed by Martinez et al [5]. For the major part of the study, a deceleration of 0.8 g is applied to the vehicle models. In order to consider the brake dive the vehicle front is inclined by 2.5 degrees. This scenario represents accidents where the braking is initiated prior to the initial contact.

TABLE 1
GEOMETRICAL PARAMETERS OF VEHICLE CLASS REPRESENTATIVES

Vehicle Model	BLE Height [mm]	Bonnet Angle [°]	Angle Bonnet-Windscreen [°]	WAD [mm]
Compact	777	18.5	173	1522
Sedan	763	11.3	161.3	1877
Van	775	21.8	172.2	1607
Sports Car	532	16.2	166.7	1812
SUV	955	13.4	163.9	1793
OneBox	1021	31.2	172.7	1550

The kinematics is determined by simulations with the MADYMO multi-body solver, taking collision speeds of 20, 30, 35 and 40 km/h into account. The collision speed corresponds to the vehicle speed at the time of the initial contact between pedestrian and vehicle. The simulated scenario is based on accident research data and describes a pedestrian crossing in front of a vehicle, i.e. the pedestrian models are configured facing sideways to the vehicle. Beside different adult pedestrian models (5th percentile female, 50th percentile and 95th percentile male) a 6-year-old child model is also considered (Table 2). Those four models cover a wide spectrum of possible pedestrian heights. In the following, a general differentiation between children and adults will be made. For this study the 6 year old child and the 5th percentile female are assigned to the group of children, whereas the 50th percentile male and the 95th percentile male represent the group of adults.

TABLE 2
MADYMO PEDESTRIAN MODELS

	6 year old child	5th percentile female	50th percentile male	95th percentile male
Height [m]	1.17	1.53	1.74	1.91
Weight [kg]	23.0	49.77	75.7	101.1
CG height [mm]	665.6	843.8	958.9	1075.3

For each pedestrian model two walking postures are considered with the leg facing the vehicle backward and forward respectively (Fig. 3). The kinematic analysis is focused on a centred impact position of the pedestrian. In order to examine the sensitivity of a centred impact, four additional positions are defined, located 50 and 100 mm to the left and right of the longitudinal vehicle axis (Fig. 4). There is no initial velocity applied to the pedestrian models. The defined boundary conditions have been previously validated by reconstruction of two real-world accident cases [6]. The impact locations of the different body parts at the vehicle front as well as the longitudinal and lateral throw distances could be reproduced within the corresponding simulations.
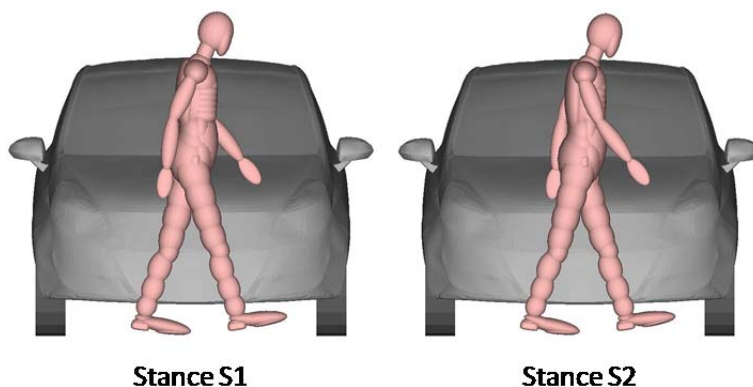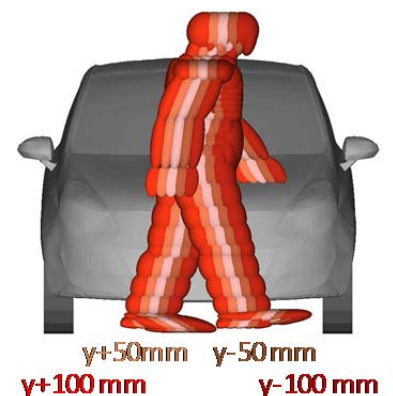
Fig. 3. Stances

Fig. 4. Five impact positions

The consideration of six vehicle front geometries, four pedestrian models, four collision speeds, five impact positions and two walking postures adds up to a total of 960 simulations, forming the major part of the study.

Experimental Testing

Tests with the Polar-II pedestrian dummy from Honda, which have been conducted by fka in cooperation with the German Insurers Accident Research (UDV) and published by Hamacher et al [7], demonstrate, among other things, the influence of a reduction in collision speed on pedestrian kinematics. Although the focus of those tests has been on primary impact, conclusions regarding post-car impact pedestrian kinematics can be drawn

within the current publication. The experimental vehicle represents an average front design with a high relevance in road traffic and it is designed to current pedestrian safety standards. Three tests are presented in this paper, carried out at collision speeds of 40, 30 and 20 km/h. The test setup (Fig. 5) corresponds to the general accident scenario defined within the simulations, i.e. a pedestrian crossing in front of a vehicle. The dummy is positioned centred in walking posture with the head orientated perpendicular to the driving direction of the experimental vehicle. The leg facing the vehicle is backwards and the wrists are tightly bound. The adjustment of the dummy is carried out according to the posture and the joint alignments respectively given in [8] and therefore differs from the stances defined within the simulations. The secondary impact itself cannot be assessed since the ground is covered with Styrofoam plates in order to protect the dummy from damage (Fig. 6). Furthermore, the sliding distance of the dummy is limited due to a safety net, which is mounted 12 m behind its initial position.
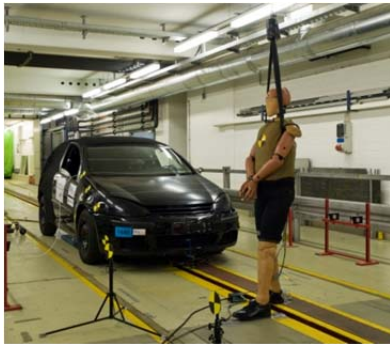

Fig. 5. Test setup

Fig. 6. Ground impact conditions

The Honda Polar-II dummy has been specially developed and validated for the performance of full-scale tests and is supposed to reproduce the kinematics and loadings of a 50 %-male during a vehicle-pedestrian collision [8]. The dummy is connected via a belt with a release mechanism, which is activated by a trigger. This happens ca. 50 ms prior to the impact, so that the dummy is free-standing at the time of contact with the vehicle. After the primary head impact a full braking of the vehicle is initiated, corresponding to the recommendation in [8].

III. RESULTS

In the following, several kinematic parameters are examined, resulting in a qualitative assessment of the different vehicle class representatives regarding secondary impact. In the first section of the results the pedestrian kinematics within the different phases of the pedestrian accident is generally described using three scenarios out of the performed simulations.

Overall Pedestrian Kinematics

The pedestrian kinematics can be illustrated by the motion of the centre of gravity (CG). The curve shown in Fig 7 represents the z-component of the centre of gravity position.
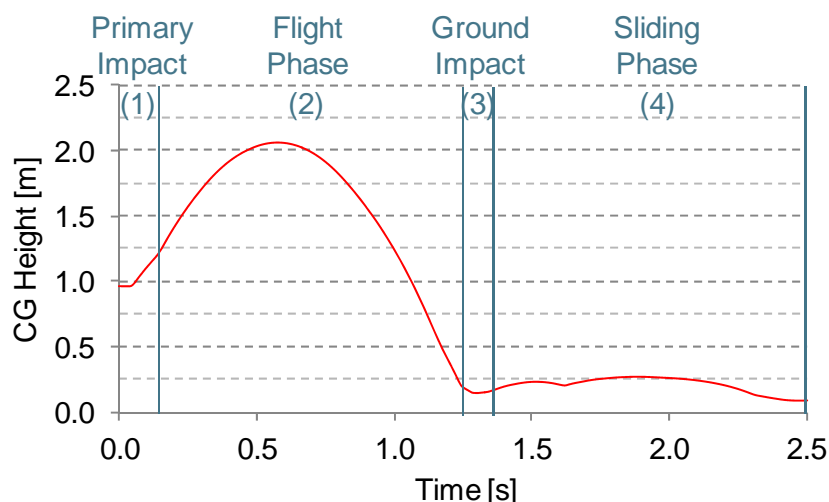

Fig. 7. CG height during the phases of pedestrian accident (Compact, 50th percentile male, S1, 40 km/h)

The different phases of the pedestrian accident are marked by vertical lines. The first increase is attributed to the impact of the torso on the bonnet. The pedestrian is accelerated mainly in x- and z-direction due to the impact momentum. The primary impact ends with the head impact, marked by the second increase, which at the same time indicates the time of disengagement of the pedestrian from the vehicle. The pedestrian centre of gravity velocity reaches a maximum here.

The flight phase is described by a trajectory parabola. The fall distance, marked by the maximum of the parabola, is higher than the distance the pedestrian centre of gravity has travelled in vertical direction before it reaches the maximum. In general the velocity tends to be higher when ground impact is imminent than at the beginning of the flight phase, due to the gravitational acceleration of the pedestrian during his fall.

In case of a secondary impact on the car the pedestrian is carried on the vehicle for a certain distance until he is finally disengaged from the vehicle. In Fig. 8 such behaviour is illustrated for a 50th percentile male, who collides with a sports car at a speed of 40 km/h. At a flight altitude of 1.5 m he is hit again by the car before he finally disengages ca. 1 s after the initial contact. Thereby the potential energy due to the flight height is dissipated in two steps, which should be beneficial with respect to the vertical impact with the ground. Furthermore, the stiffness of the road surface is generally higher than for the vehicle front.
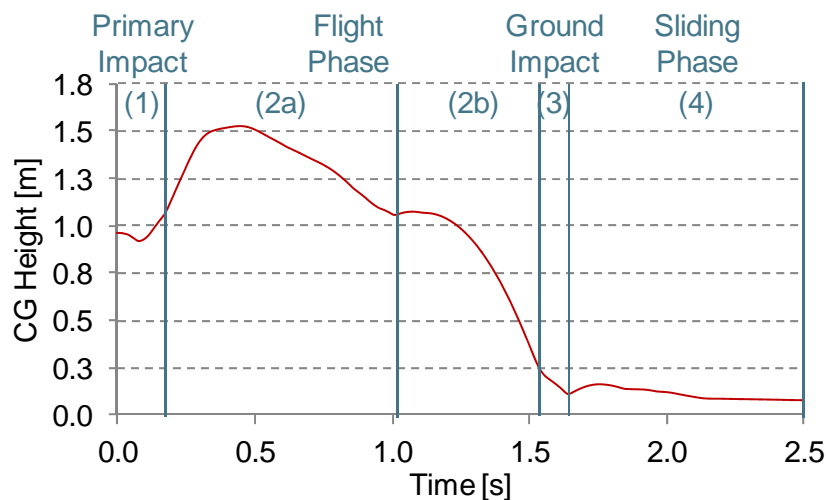
Fig. 8. CG height during the phases of pedestrian accident (Sports Car, 50th percentile male, S2, 40 km/h)

In the ground impact phase the pedestrian is decelerated. The deceleration level depends on the angular position of the pedestrian at the time of impact, i.e. which part of the body impacts first. In case the extremities hit the ground first the deceleration is at first comparatively low, as it is the case in Fig 8. As soon as the torso and the head respectively impact, the centre of gravity deceleration is higher. In Fig. 8 this becomes apparent by the minimum at ca. 1.65 s, which marks the end of the ground impact phase. Fig. 9 illustrates the curve for a scenario where the head impacts first. In contrast to Fig. 8 there is an abrupt deceleration resulting in a curved minimum for the CG height. Hence, the curve progression around the minimum gives information about whether the initial ground contact happens with a stiff body region or not.
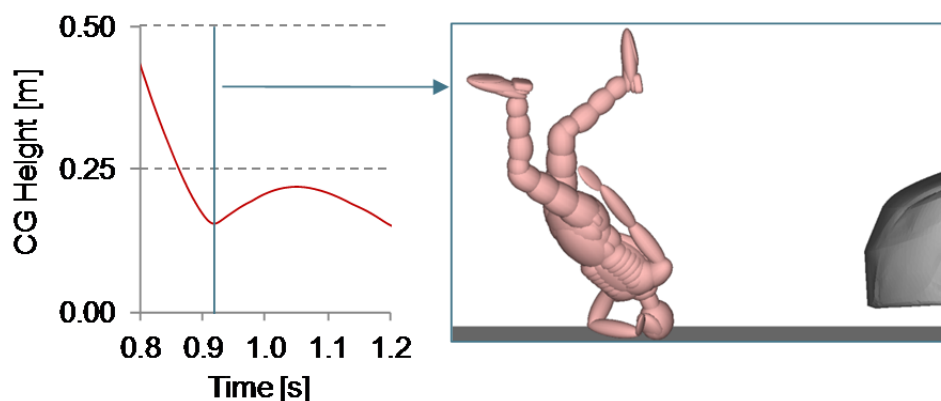
Fig. 9. Ground impact with initial contact of the head (Compact, 50th percentile male, S1, 20 km/h)

The portion of kinetic energy that is not absorbed during the ground impact is dissipated in the sliding phase. After the height of the centre of gravity has reached a minimum due to the ground impact, a momentary rebound movement usually occurs. As soon as it has faded, the pedestrian performs a pure sliding and rolling movement until he comes to rest at his final position. The kinematic boundary conditions before the ground impact affect the development of repeated landings during the sliding phase and therefore influence the sliding distance.

Flight Altitude

For the classes Compact, Van, SUV and OneBox the stance of the pedestrian as well as the defined variation of impact positions have rather little influence on the flight altitude. In Fig. 10 and Fig. 11 the average values for the flight altitude reached by the particular pedestrian models are illustrated for the group of children.
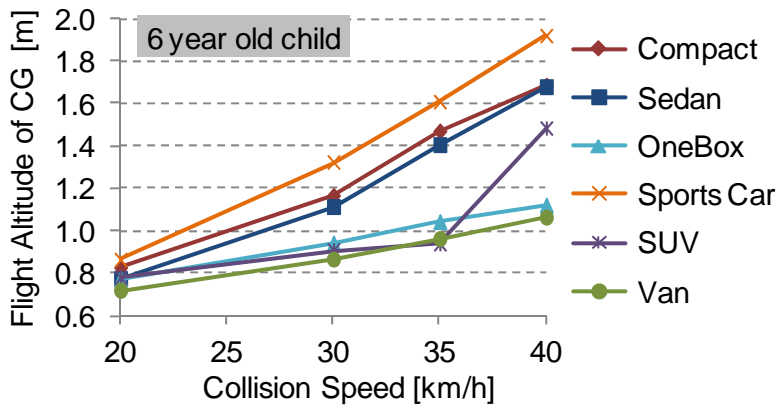

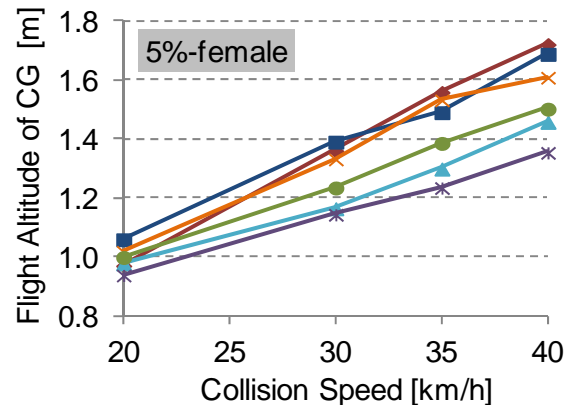Fig. 10. Average flight altitude of 6 year old child

Fig. 11. Average flight altitude of 5th percentile female

It becomes apparent that for children, independent from the collision speed, the classes OneBox, Van and SUV possess lower values compared to the other classes. This behaviour arises from the steep front geometry of those vehicles as well as the high bonnet leading edges of the SUV and OneBox classes. The scenario of an SUV hitting the 6 year old child at a collision speed of 40 km/h is conspicuous (Fig. 10). Here there is a great effect of the pedestrian stance on the flight altitude due to limitations of the MADYMO pedestrian model. Within the animations it was observed that the joints reached the limit of their range of motion. This seems to be the main cause for the differing flight altitude. Depending on the direction of rotation around the pedestrian's z-axis, the model's joints were more or less flexible. This led to completely different flight parameters, as it is the case for stance S1 and S2 in the scenario of a SUV hitting the 6 year old child.

The average flight altitudes for the group of adults are displayed in Fig. 12 and Fig. 13. The values of the 50th percentile and 95th percentile male are quite similar for the particular vehicle classes. Due to their height the influence of the front geometry on the flight altitude is lower than for the children.
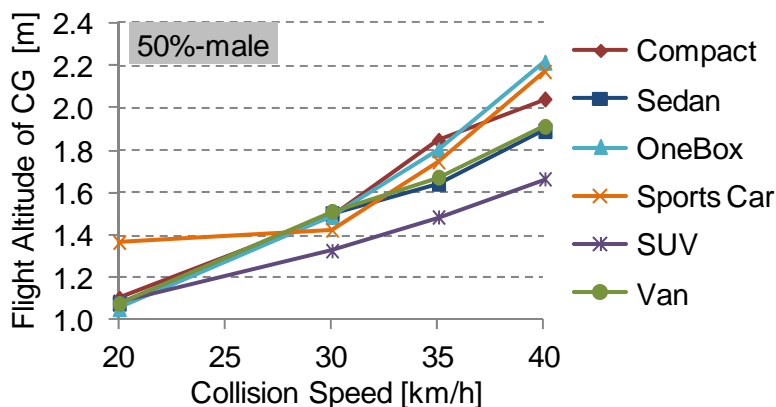

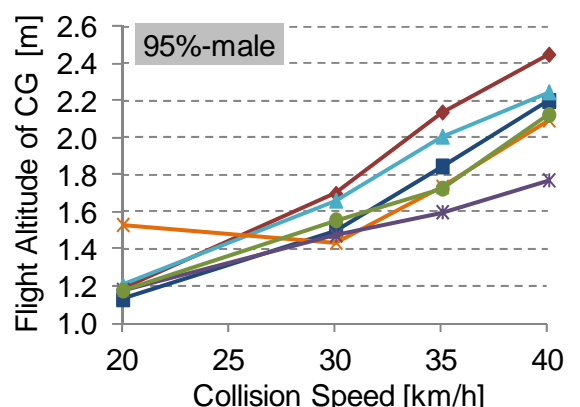Fig. 12. Average flight altitude of 50th percentile-male

Fig. 13. Average flight altitude of 95th percentile male

While for short pedestrians the BLE area significantly affects the pelvis kinematics and acts as a pivotal point for further movement, tall pedestrians do not show such a drastic change from pelvis contact with the vehicle front. Here, in the case of a vehicle with regular BLE height, the pelvis just goes over the bonnet. In contrast to the other vehicle classes the sports car shows no clear decrease of the flight altitude for a collision speed of 20 km/h. The low BLE height, together with the flat bonnet angle, leads to a great launch angle. Thus, comparatively high flight altitudes are reached even for low collision speeds, emphasising the significance of this kinematic parameter.

Throw Distance

In Fig. 14 and Fig. 15 the average throw distances for the 6 year old child as well as the 5th percentile female are illustrated. The sports car causes the highest flight altitude for the children and at the same time the lowest throw distance. On the contrary, the OneBox vehicle causes the longest throw distances while the flight altitude is quite low. The steep front geometry of this vehicle, which possesses the highest BLE as well as the largest bonnet angle of all vehicle fronts in the study, leads to an early head impact and implicates a momentum transfer that is mainly oriented parallel to the ground whereas the vertically oriented component of the transferred momentum is negligible.
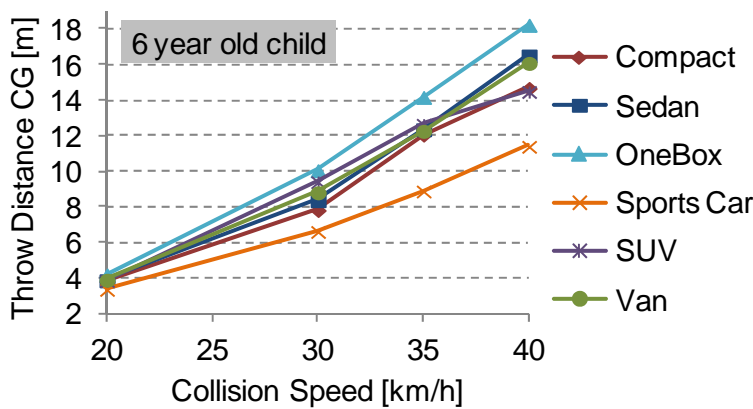
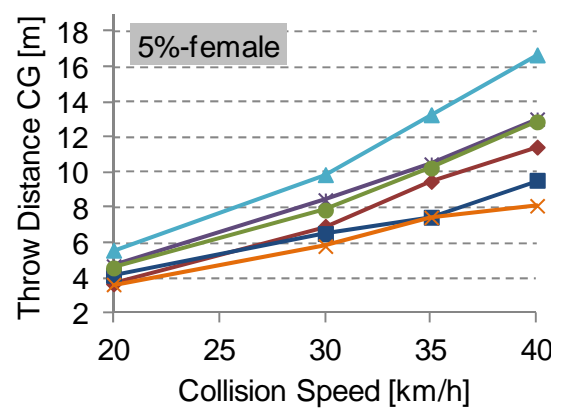Fig. 14. Average throw distance of 6 year old child

Fig. 15. Average throw distance of 5th percentile female

The group of the adults, in comparison to the children, does not show the same trend with respect to the throw distance. Contrary to the previous observations, which showed that a low flight altitude is related to a large throw distance, the OneBox vehicle causes high flight altitudes as well as high average throw distances. The same applies also to the sports car at a collision speed of 20 km/h.
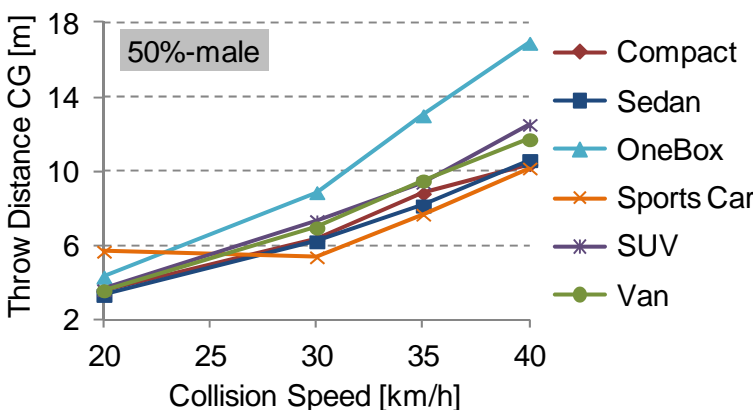
Fig. 16. Average throw distance of 50th percentile male
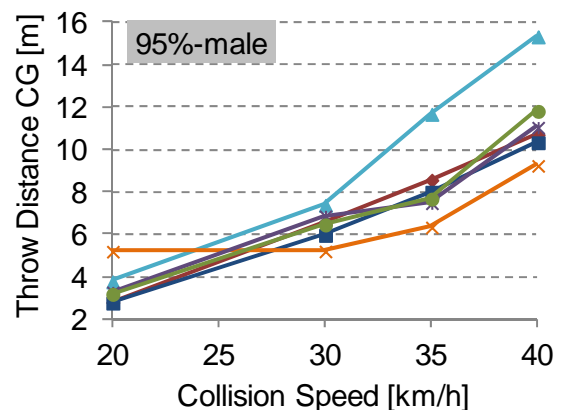
Fig. 17. Average throw distance of 95th percentile male

A large throw distance does not rank among the main injury causations but it increases the probability for a tertiary impact with infrastructure. A short throw distance, however, may lead to a run over of the pedestrian in cases where the vehicle deceleration is too low. With regard to the minimum throw distances determined for

each collision speed, a deceleration below 1 m/s² would be sufficient to stop the vehicle in time. Thus, there is a relatively modest risk for a run over, as observed in practice as well [9].

Launch Speed

Both launch speed and launch angle are derived from the CG velocity and influence the trajectory shape during the flight phase. Fig. 18 and Fig. 19 show an overview of the average launch speeds of the child models. It is conspicuous that the launch speed of the 6 year old child in some cases turns out higher than the collision speed. Beside the low weight of the child model, the short durations of the primary impact measured for the classes OneBox, SUV and Van contribute to a high launch speed since the vehicle loses comparatively little speed until the head impact. The sports car possesses the highest head impact times, along with the lowest launch speeds. In the case of the 5th percentile female the spread of launch speeds is similar but ranges on a lower level, which seems to be a consequence of the increased primary impact durations compared to the 6 year old child.
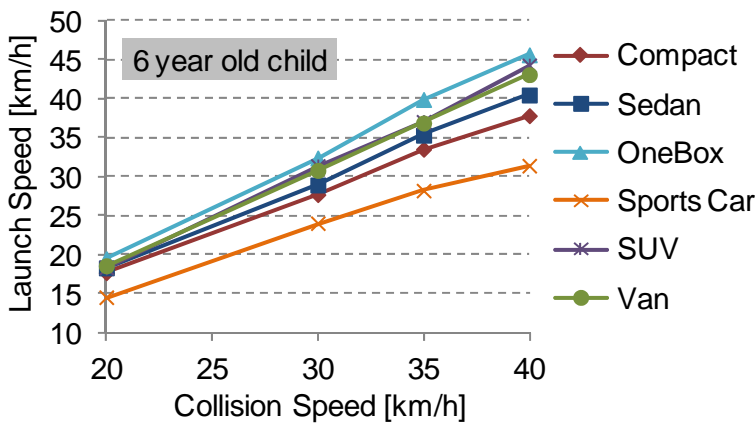

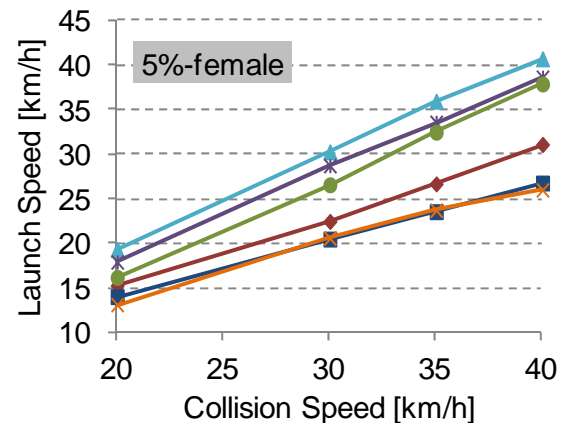Fig. 18. Average launch speed of 6 year old child

Fig. 19. Average launch speed of 5th percentile female

The launch speeds of the adults are illustrated in Fig. 20 and Fig. 21. The values further decrease compared to the group of children and for all vehicle classes lie below the collision speed. As for the previous parameters the sports car shows a deviant behaviour at a collision speed of 20 km/h.
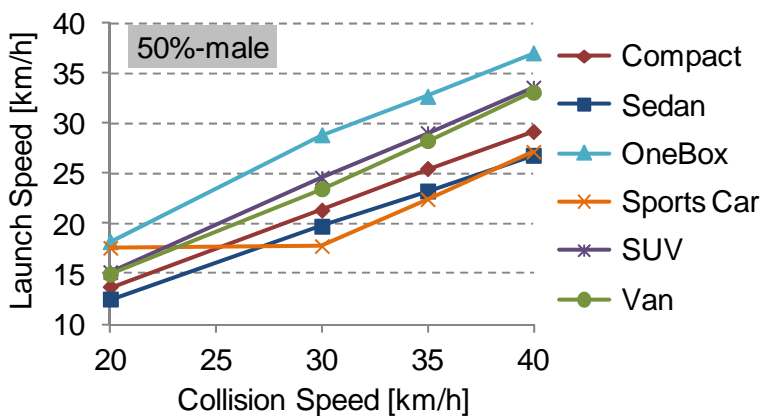
Fig. 20. Average launch speed of 50th percentile male
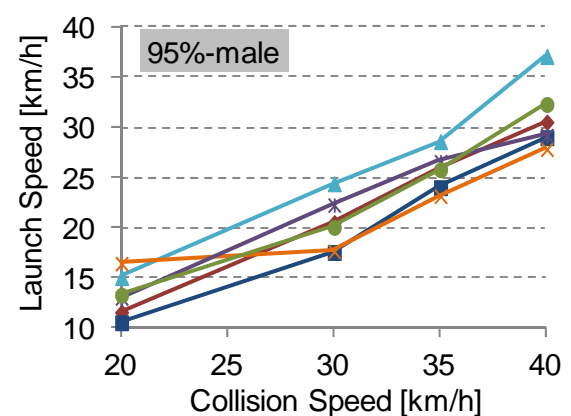
Fig. 21. Average launch speed of 95th percentile male

With respect to the secondary impact a low launch speed is beneficial since it goes along with a reduced amount of impact energy (quadratic relationship). The sports car receives the highest rating for this kinematic parameter since it possesses the lowest values for all pedestrian models. The opposite is true for the OneBox class, which gets the poorest rating.

Launch Angle

Fig. 22 and Fig. 23 show the average launch angles for the child models. It is conspicuous that for collisions between the 6 year old child model and the SUV the launch angles, contrary to all other vehicle classes, become

smaller with increasing collision speeds. The launch angles obtained by the OneBox class reveal an untypical behaviour, too. Here the values are almost constant over the considered speed range.

Fig. 22. Average launch angle of 6 year old child
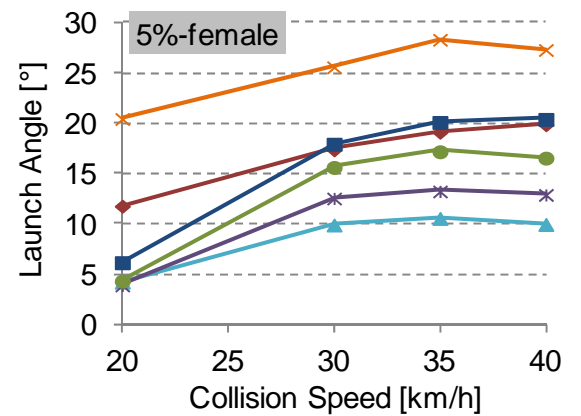
Fig. 23. Average launch angle of 5th percentile female

As already mentioned for the flight altitude, the observed behaviour is assumed to be a result of the steep front geometry of those vehicles as well as the high bonnet leading edges. In combination with the small body height of the 6 year old child the time period until the head impact occurs becomes quite short resulting in a limited rotation of the pedestrian towards the bonnet. The impact momentum is transferred more into throw distance rather than flight altitude. This leads to a reduced launch angle.

For the adults the launch angles are illustrated in Fig. 24 and Fig. 25. In comparison to the other vehicle classes the classes SUV and OneBox throw the pedestrian off in a flatter angle. The sports car achieves the highest launch angles for all pedestrian models as well as collision speeds.
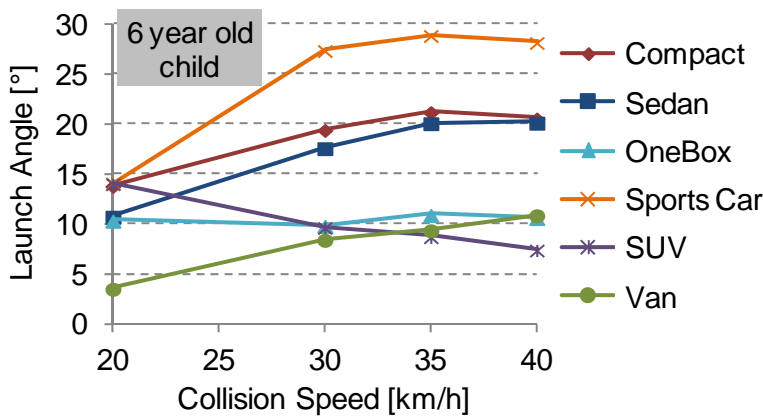

Fig. 24. Average launch angle of 50th percentile male

Fig. 25. Average launch angle of 95th percentile male

Launch angle and launch speed are reflected in the angular position of the pedestrian after the primary head impact. Fig. 26 demonstrates how a reduction in collision speed affects the post-car impact pedestrian kinematics.

Fig. 26. Polar-II dummy tests with different collision speeds (50th percentile male)

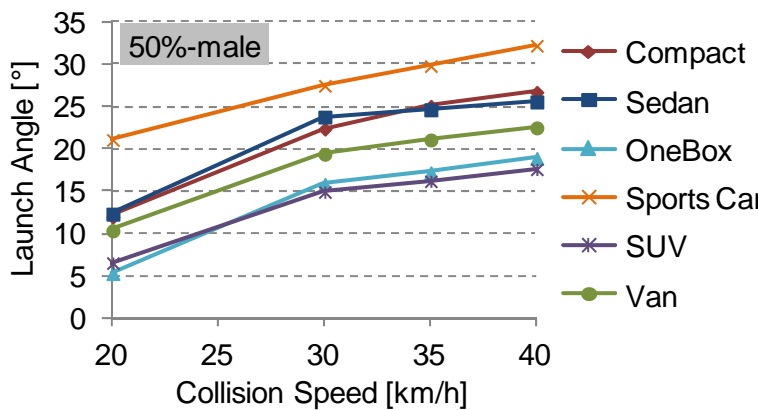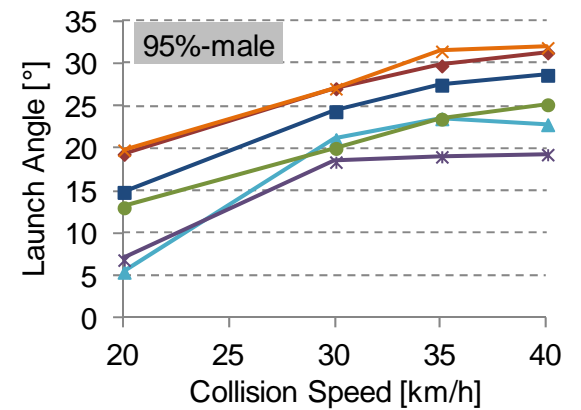The red dashed lines visualise the angular position of the dummy 400 ms after the initial contact. The rotation of the pedestrian around his sagittal axis decreases with speed. In case of the 20 km/h test the red dashed line at the same time also indicates the subsequent flight characteristics as well as direction of the dummy. Thus, the rotatory motion is reduced significantly compared to the 40 km/h test. In general the collision speed has the biggest influence on the kinematics in the flight phase as substantiated by the parameters analysed.

Rotation and Probability of an Initial Head Contact on the Ground

To assess the probability of an initial head contact on the ground, determining the rotation of the pedestrian around his transverse and sagittal axis is crucial. The simulation results indicate that the rotational velocity decreases with pedestrian height. Pedestrian stance at the time of initial contact influences the flight characteristics and in particular the rotation of the model, which makes precise predictions of the head impact risk with the ground difficult. Nevertheless, the flight characteristics identified for each vehicle class enable a general risk assessment.

Regarding the probability of an initial head contact on the ground especially the OneBox class is noticeable. In particular for the adults an initial head impact occurs in most of the simulations. Here the pedestrian model often does a half turn around his sagittal axis. For the children the rotatory motion is more distinctive, i.e. the rotation angles are higher, so that the head impact probability is not significantly higher than for the other classes. Furthermore, the effect of a flat vehicle front, as in the case of the sports car, is notable. For this vehicle class the rotation of the pedestrian is most distinctive. From the initial contact up to the ground impact the pedestrian models rotate through angles of 240° to 420° on average, which makes an initial head impact, under the given boundary conditions, comparatively unlikely.

Fig. 27 illustrates the pedestrian kinematics for the Polar-II dummy test conducted with a collision speed of 40 km/h. The dummy turns through almost 270 degrees until he impacts the ground, which confirms the distinctive rotations observed in the simulations. The shoulder strikes the ground first, followed by the head.

Fig. 27. Polar-II dummy test with a collision speed of 40 km/h (UDV, German Insurers Accident Research)

Probability of a Secondary Impact on the Vehicle

In order to analyse the probability of a secondary impact on the vehicle additional simulations with a reduced vehicle deceleration of 0.5 g (instead of 0.8 g) and without brake dive have been performed. It could be found that in the case of the sports car a secondary impact on the vehicle (Fig. 8) is most likely compared to the other classes in the study. Also for the classes Sedan and Compact a re-contact between pedestrian and vehicle front occurred comparatively often within the additional simulations. This applies particularly to the group of adults. The lowest re-impact probability is obtained for the class OneBox, followed by the classes Van and SUV. For those three classes a secondary impact on the vehicle took place in less than 20% of the simulations with reduced vehicle deceleration. This change in boundary conditions results in an increased number of simulations with a re-contact between pedestrian and vehicle front, illustrating the influence of the vehicle deceleration on the pedestrian kinematics. For comparison, the simulations with a vehicle deceleration of 0.8 g show no secondary impact on the car for the classes OneBox, Van and SUV. Especially for the group of children the probability is reduced since the centre of gravity lies quite low while at the same time all six vehicle classes possess a steep geometry below the BLE.

Vehicle-Class-Specific Assessment of Secondary Impact

The assessment of the secondary impact is based on five kinematic parameters. The parameters selected are the launch speed, the flight altitude, the throw distance, the probability of an initial head contact on the ground and the probability of a secondary impact on the vehicle. Those parameters form the assessment criteria, which are transferred into qualitative statements on secondary impact (moderate, critical, very critical) for each vehicle class as well as pedestrian group. This is done with the help of a scoring scheme. For a moderate rating within a category the corresponding vehicle class receives 2 points while for a critical rating 1 point and for a very critical rating no points are assigned. The points reached for each assessment category are added up without any weighting. Finally, the total scores achieved by each vehicle class allow a comparative assessment. Table 3 summarises the outcome of the qualitative comparison of the particular vehicle classes.

TABLE 3
QUALITATIVE COMPARISON OF THE VEHICLE CLASSES REGARDING
SECONDARY IMPACT

Vehicle Class	Children	Adults
Compact	critical	critical
Sedan	critical	moderate
OneBox	very critical	very critical
Sports Car	moderate	moderate
SUV	very critical	very critical
Van	very critical	critical

moderate (yellow)   critical (orange)   very critical (red)

   Due to the disadvantageous post-car impact pedestrian kinematics caused by the SUV and the OneBox classes, those vehicles turn out to be particularly critical. The classes Compact, Sedan and Sports Car show more favourable kinematics, as a result of the distinct pedestrian wrap around distances, which tend to cause a less critical secondary impact. This does not apply to the class Van. Here the steeper bonnet angle affects the results adversely.

IV. DISCUSSION

   In this comparative study emphasis is placed on general trends in post-car impact pedestrian kinematics derived out of multibody simulations with six different vehicle front geometries. The values presented are strongly related to the boundary conditions defined and to some extent affected by the limitations of the MADYMO pedestrian model, which is not validated for an analysis of secondary impact. The limitations of the MADYMO pedestrian model are exemplified by the case of the 6-year-old child colliding with the SUV front geometry. Within the animations it was observed that the joints reached the limit of their range of motion. Depending on the direction of rotation around the pedestrian's z-axis, the model's joints were more or less

flexible. This led to completely different flight parameters. Nonetheless, a qualitative comparison between the vehicle classes can be made and reveals the influence of different modern front shapes on pedestrian kinematics. Due to the great amount of simulations within the study the general trends indentified for the given boundary conditions are sufficiently proven.

This paper deals mainly with the kinematics in the time span between primary and secondary impact. The investigated parameters have been chosen such that the severity of ground impact injuries can be estimated based on physical and biomechanical principles. For thorough examination of ground contact mechanisms, an indirect method as used in this study may be not the most suitable approach, and additional investigation of ground impact mechanisms was out of the scope of this study.

The advantage of this method, in comparison to a thorough investigation of ground impact mechanisms, is that a much more direct link can be established between the vehicle front geometry and the kinematic conditions of the pedestrian just before ground impact. Additionally, strong indications have been found that the centre of gravity kinematics provide an estimation of which body part impacts the ground first, which the authors believe is one of the key issues to address when investigating ground impact. In order to simplify future data analysis, it could be useful to establish a threshold which allows for a decision if a head impact occurred based on centre of gravity deceleration at ground impact.

The presented study was conducted independently from the one published by Simms et al [4]. Nevertheless the methods to analyse the post vehicle-impact kinematics as well as the findings are partially similar to those reported in [4]. Due to the increased simulation effort those findings could be confirmed for a wider velocity (20 - 40 km/h) as well as pedestrian (children and adults) range. Simms et al already pointed out that high fronted vehicles are disadvantageous for the post vehicle-impact kinematics. The current study shows that this is valid for children as well, who moreover have to be assessed critically with regard to the vehicle class Van.

V. CONCLUSIONS

The intention of this study is to generally assess the injury risk due to secondary impact solely with the help of kinematic parameters. With regard to the simulations performed the launch angle and speed as well as flying height are rather stable against variations of the initial stance and impact position. In contrast to this, it became apparent that the pedestrian's rotation is highly influenced by leg and arm posture, which makes precise predictions of head impact risk in secondary impact difficult. The kinematic boundary conditions before the ground impact affect the development of repeated landings during the following sliding phase and therefore influence the sliding distance. This contributes to varying throw distances.

Decisive for the kinematics is the ratio or the initial impact point at the vehicle to the centre of gravity height of the pedestrian as well as the overlap of pedestrian and vehicle due to the height of the bonnet leading edge. A head impact on the ground is most likely after an impact with an OneBox-shaped vehicle, compared to the other vehicle geometries considered in this study. A high bonnet leading edge in relation to the pedestrian stance as well as large bonnet and windshield angles contribute to this effect. On the contrary, a low BLE and small bonnet and windshield angles, as seen for sports cars, lead to a high rotational component during the flight phase. In general, late head impacts induce more variation of the analysed parameters, and initial leg and arm posture become more important.

Due to the disadvantageous post-car impact pedestrian kinematics caused by the SUV and the OneBox classes, those vehicles turn out to be particularly critical. The classes Compact, Sedan and Sports Car show more favourable kinematics with respect to the secondary impact. This does not apply to the class Van. Here the steeper bonnet angle affects the results adversely.

In general a reduction in collision speed is beneficial for the pedestrian kinematics within the simulations and leads to a decrease in altitude, rotation and throw distance. Overall, the probability of an initial head contact as well as the contact forces during head impact is reduced. Hence, a reduction in collision speed, e.g. due to an emergency brake system with pedestrian detection, forms an effective measure to minimise the injury risk coming from secondary impact.

VI. REFERENCES

[1] Grünert J, Hardy, R N, Neal-Sturgess, C, Joonekindt, S, Yang, J, Yao, J F, et al., Assessment of the relevance of the secondary (ground) impact and its influence on injuries, *APROSYS document AP-SP32-010R, Deliverable D3.2.4, 2007*

[2] Otte D, Pohlemann T, Analysis and load assessment of secondary impact to adult pedestrians after car collisions on roads, *Proceedings of IRCOBI Conference, Isle of Man, United Kingdom, 2001.*

[3] Paas R, Einfluss der Fahrzeugfrontgeometrie auf den Sekundäraufprall bei Fahrzeug-Fußgänger-Kollisionen, *Diploma Thesis, WA 1873, Institut für Kraftfahrzeuge RWTH Aachen University, December 2010*

[4] Simms, C K, Ormond, T, Wood, D P, The Influence of Vehicle Shape on Pedestrian Ground Contact Mechanisms, *Proceedings of IRCOBI Conference, Krakow, Poland, 2011*

[5] Martinez, L, Guerra, L J, Ferichola, G, Garcia, A, Yang, J, Yao, J F, Stiffness Corridors for the Current European Fleet, *APROSYS document AP-SP31-009R, Deliverable D3.1.2.B, 2006*

[6] Hamacher, M, Fußgängerschutz am Kraftfahrzeug, *Final Report Project 85210, Forschungsgesellschaft Kraftfahrwesen mbH Aachen, December 2010*

[7] Hamacher, M, Eckstein, L, Kühn, M, Hummel, T, Assessment of Active and Passive Technical Measures for Pedestrian Protection at the Vehicle Front, *Proceedings of ESV Conference, Paper Number 11-0057, Washington, DC, 2011*

[8] Surface Vehicle Recommended Practice, *SAE International Document J2782, Performance Specifications for a 50th Percentile Male Pedestrian Research Dummy, 2007*

[9] Liers, H, Hannawald, L, Klassifizierung von Fahrzeugfrontkonturen in Fußgängerfrontalunfällen, *VUFO - Verkehrsunfallforschung an der TU Dresden GmbH, June 2008*